International Conference on Space Optics—ICSO 2018

Chania, Greece

9–12 October 2018

Solar rejection window and narrow band pass filters for the Meteosat third generation lighting imager

C. Montcalm

A. Badeen

D. Burbidge

R. Bruce

et al.

Solar Rejection Window and Narrow Bandpass Filters for the Meteosat Third Generation Lightning Imager

C. Montcalm[1a], A. Badeen[a], D. Burbidge[a], R. Bruce[a], G. Carlow[a], J. Dane[a], N. Firdawsi[a], G. E. Laframboise[a], A.M. Miles[a], J.-P. Noel[2a], R. Rinfret[a], B.T. Sullivan[a], R. Bardazzi[b], S. Lorenzini[b], and L. Giunti[b]

[a]Iridian Spectral Technologies, Ottawa, Ontario, Canada; [b]Leonardo S.p.A., Florence, Italy.

ABSTRACT

This paper presents the design, manufacture and characterization results of two optical interference filters to be used in the Lightning Imager (LI) optical head on the Meteosat Third Generation (MTG) mission. The first optical filter is a Solar Rejection Window (SRW) to limit the solar thermal radiation absorbed by the optical head while the second optical filter is a Narrow Band Filter (NBF) intended to only pass the lightning discharge emission wavelengths.

Each filter has its own distinctive design considerations and manufacturing challenges. The SRW must pass wavelengths from the 760 to 780 nm spectral range and reject (block) wavelengths from the ultraviolet (UV) to the mid-wave infrared (MWIR) and up to 16.3° angle of incidence (AOI) and over a large temperature range (as when exposed to direct sunlight).

The NBF is designed to pass only the oxygen emission triplet, centered around the 777.6 nm (vacuum) wavelength and rejecting other wavelengths. Considering the AOI of the light and the temperature excursion, the center wavelength (CWL) uniformity has to be better than 0.04% peak-to-valley (PV) over the 114 mm diameter clear aperture, which is a formidable challenge. We achieved a coating thickness uniformity less than ±0.01% PV, exceeding the prescribed specification. Post-deposition annealing was carried out to tune the bandpass to within pico-meters (pm) of the target CWL value while maintaining the desired CWL uniformity.

To ensure that both the SRW and NBF filter meet the desired optical and physical specifications, a comprehensive series of optical and physical characterization tests, along with durability tests, were carried out on each deposition batch.

Keywords: Narrow bandpass filter, solar rejection window, multilayer coatings, coating uniformity, space qualified

1. INTRODUCTION

The Meteosat Third Generation (MTG) Mission is the Operational Geo-Stationary Meteorological system that will replace the Meteosat Second Generation System (MSG) at the end of its operational life [Ref. 1 and 2]. MTG, in a geostationary orbit at an altitude of 36,000 km, is designed for the accurate prediction of meteorological phenomena and the monitoring of climate and air composition through operational applications for the period of time from 2021 onward. The MTG mission lifetime is 8.5 years in-orbit, following a ground lifetime including AIV, testing and storage of 4 years for the first platform and 17 years for the last platform.

The Lightning Imager (LI), part of MTG-I satellite, is tasked with the mission to continuously detect lightning discharges taking place in clouds or between cloud and ground with a spatial footprint of ~10km radius over almost the full Earth disc. The primary objective of the LI mission is to provide full radiometric information relevant to the detection and location of cloud-to-ground and cloud-to-cloud lightning in addition to those provided by existing/planned ground-based lightning detection systems, so to overcome their limited coverage. This continuous recording of lightning over the whole hemisphere will provide a new set of data useful in nowcasting, climatology and atmospheric research.

Thales Alenia Space, as the MTG programme and MTG-I satellite prime contractor, is responsible for the procurement of the LI Instrument developed and manufactured by Leonardo S.p.A. Leonardo has contracted Iridian Spectral

---

[1] claude.montcalm@iridian.ca; phone +1-613-741-4513; fax +1-613-741-9986; www.iridian.ca
[2] J. P Noel is now with the Institute for Microstructural Sciences, National Research Council of Canada, Ottawa, Ontario, Canada.

Technologies Ltd. for the design and fabrication of a solar rejection window (SRW) optical filter and a narrow bandpass optical filter (NBF) to be used in the LI. This paper describes the requirements of these two optical filters and present the results of characterization and environmental robustness testing.

2. INSTRUMENT OPTICAL SYSTEM OVERVIEW

The LI instrument requirements, shown in **Table 1**, are challenging and they define, together with the concept adopted for the lightning detection, the main drivers for the LI design. The LI is composed of an optical head and associated electronic equipment. A schematic of the LI optical head is shown in Figure 1.

The LI optical head consists of four identical optical channels, each one including:

- a baffle for stray light suppression and thermal load minimization
- a SRW to minimize both the background level and the thermal load inside the optical channel
- a NBF to pass only the lightning spectral pulse (777.41, 777.63 and 777.75 nm nm)
- an optical system with F#1.73, a 110 mm entrance pupil diameter (determined by radiometry required to achieve the instrument average detection probability performance) and a 191 mm effective focal length (determined by the targeted ground sampling distance of 4.5 km at sub-satellite point and the size of detector pixels)
- a CMOS detector with 1000 x 1170 pixels, 24 μm pitch, 1000 frame per second
- a processing electronics implementing the detection functions

Each optical channel images a different portion of the visible Earth surface with four line of sights tilted about 5° from the sub-satellite point toward North, South, West and East in order to achieve the required coverage.

A multi-channel architecture was chosen with the NBF positioned in the entrance pupil to ensure light is incident at a near normal angle (parallel beam) that optimizes the NBF performance while reducing the optical assembly and detector size [3]. The NBF parallel beam concept also improves the signal-to-noise ratio, both in night and daylight conditions. In addition, the pupil diameter was set to 110 mm to maximize the instrument average detection probability, reduce the NBF uniformity requirements and limit the mass, envelope, and complexity of the optical system.

Each optical channel has an independent single stage lens, detector and baffle, with an effective focal length of 190.8 mm, an entrance pupil diameter of 110 mm and a 5.1° field of view (Figure 1). The SRW and the NBF, both 130 mm in diameter but with effective apertures of 120 and 114 mm diameter, respectively, are the first two parallel plates in the layout schematic followed by the five lenses (all spherical except for one) of the imager. The physical diameter of each of the filters and lenses is sized larger such that "light traps" can be added at the edges to capture the straylight.

Table 1 - Lightning Imager (LI) Requirements

Parameter	Requirement
Field of view (FOV)	16° diameter shifted northward or 84% of visible Earth disk, including all Eumetsat member states
Spatial sampling	< 10 km @ latitude 45° and subsatellite longitude
Dynamic range of Earth background	0 - 500 W/m^2/μm/sr (night - top of clouds midday)
Optical pulse dynamic range	6.7 - 670 mW/m²/sr
Optical pulse spectral range	O$_2$ discharge triplet: λ1 = 777.41 nm, λ2 = 777.63 nm, λ3 = 777.75 nm
Minimum optical pulse duration	0.6 msec
Optical pulse size	10 km - 100 km circular pulsed diameter
Maximum number of optical pulses in the FOV	25 in 1 msec and 800 in 1 sec
Average Detection Probability at L1b output	70% for latitude 45° 70% as average over the FOV 40% over EUMETSAT member states
FAR (False Alarm Rate) at L1b output	< 35000/s
LI mass (total optical head and electronic box)	93 kg
LI optical head envelope	718 x 1200 x 1456 mm^3
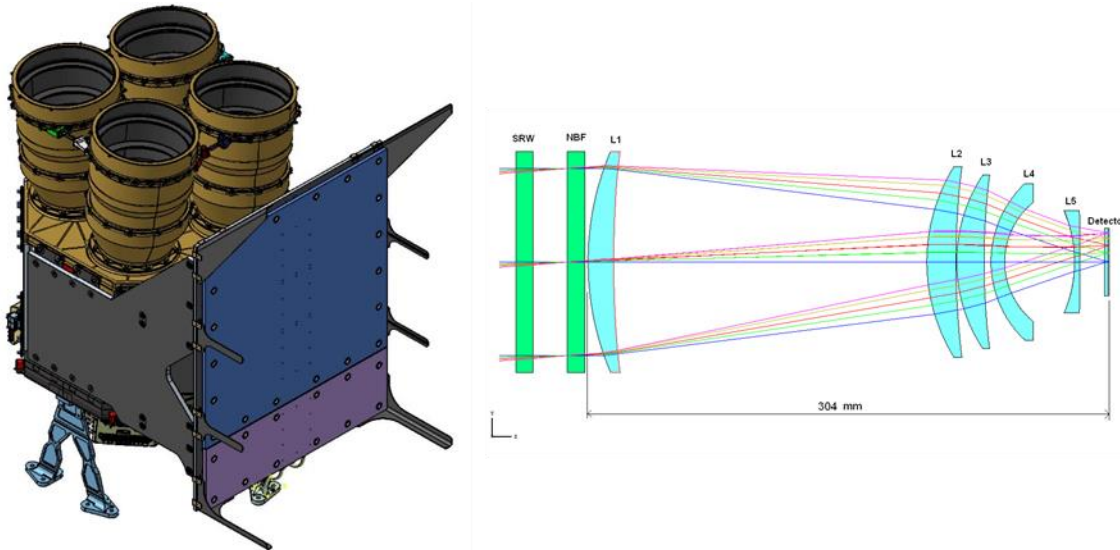
Figure 1 - Lightning imager rendering and optical system layout

3. SRW AND NBF FILTER REQUIREMENTS

The SRW is designed to reflect the solar radiation but pass the lightning discharge spectral region and it is directly exposed to the external space environment. It works in synergy with the NBF to obtain the required spectral filtering but its mechanical mounting is thermally decoupled with respect the NBF and the rest of the optical system. Consequently, the temperature excursions experienced by the SRW is much larger than the rest of the optical system.

3.1 SRW requirements

In **Table 2**, the optical performance requirements for SRW are listed in terms of transmittance at the scientific (lightning) band and the SRW Total Energy Transmitted (TET_{SRW}), Reflected (TER_{SRW}) and Absorbed (TEA_{SRW}) values corresponding to the transmitted, reflected and absorbed energy in the 200 to 2000 nm spectral range are calculated as follows:

$$TET_{SRW} = \frac{\int_{200}^{2000} S(\lambda) * T_{SRW}(\lambda) d\lambda}{\int_{200}^{2000} S(\lambda) d\lambda} \tag{1}$$

$$TER_{SRW} = \frac{\int_{200}^{2000} S(\lambda) * R_{SRW}(\lambda) d\lambda}{\int_{200}^{2000} S(\lambda) d\lambda} \tag{2}$$

$$TEA_{SRW} = \frac{\int_{200}^{2000} S(\lambda) * A_{SRW}(\lambda) d\lambda}{\int_{200}^{2000} S(\lambda) d\lambda} \tag{3}$$

where $S(\lambda)$ is the Planck distribution for an equivalent black body at 5780°K.

The SRW filter must additionally be designed to minimize the ghost generation in the 777.41 – 777.75 nm range for all angles between 0 and 16.3°, as well as minimizing the polarization sensitivity (Table 2). The ghost generation (*Ghost1*), defined by Eq. 4, is caused by internal reflections between the filter surfaces where R_A and R_B are the average reflection coefficients of the A and B filter surfaces.

$$Ghost1 = R_A \times R_B \tag{4}$$

The polarization sensitivity (*PS*), is defined as follows (same equation for the NBF).:

$$PS = \frac{\int_{772.4}^{782.4} T_p(\lambda)d\lambda - \int_{772.4}^{782.4} T_s(\lambda)d\lambda}{\int_{772.4}^{782.4} T_p(\lambda)d\lambda + \int_{772.4}^{782.4} T_s(\lambda)d\lambda} \tag{5}$$

Table 2 - SRW optical performance and ghost minimization requirements. All requirements must be met up to 16.3° AOI, except the polarization sensitivity that is limited to 5.1°.

Parameter description	Wavelength range (nm)	Value
Transmittance	774.41 – 777.75	>97%
Total Energy Transmitted (TET_{SRW})	200 – 2000	<10%
Total Energy Reflected (TER_{SRW})	200 – 2000	>85%
Total Energy Absorbed (TEA_{SRW})	200 – 2000	<5%
Average Energy Transmitted (AET_{SRW})	2000 – 10000	<5%
Average Energy Reflected (AER_{SRW})	2000 – 10000	>8%
Average Energy Absorbed (AEA_{SRW})	2000 – 10000	<87%
SRW Ghost1	774.41 – 777.75	<0.03%
SRW Reflectance side A	775 - 780	<1.5%
SRW Reflectance side B	775 - 780	<1.5%
SRW Polarization sensitivity	772.4 – 782.4	<0.5%

Table 3 - NBF optical performance, ghosting and polarization sensitivity requirements. All parameters must be met up to 5.1° AOI.

Parameter description	Wavelength range (nm)	Value
NBF Weighted Transmittance (T_{NBF})	774.41 – 777.75	>87%
NBF Equivalent Bandwidth (EB_{NBF})	772.4 – 782.4	<1.94
NBF Ghost1	774.41 – 777.75	<0.03%
NBF Reflectance side A (NBF side)	775 - 780	<10%
NBF Reflectance side B (AR side)	775 - 780	>0.3%
NBF Polarization sensitivity	772.4 – 782.4	<3.5%

where $T_p(\lambda)$ and $T_s(\lambda)$ are the filter transmittance for the p- and s-polarization at any given λ.

It is critical that the SRW can survive temperatures from -100°C to +150°C and meet all optical performance specifications in Table 2 over the -10°C to +70°C temperature range, in vacuum.

3.2 NBF requirements

The NBF, placed between the SRW and the first lens, performs the spectral discrimination of the lightning pulse from the Earth background radiance. It is supported by the lens mounting system so its operative thermal range is the same as the rest of the optical system.

Table 3 shows the NBF optical performance and ghosting requirements. The transmittance in the scientific band (T_{NBF}) is defined as follows:

$$\overline{T_{NBF}} = T_{NBF}(\lambda_1) \cdot 0.47 + T_{NBF}(\lambda_2) \cdot 0.33 + T_{NBF}(\lambda_3) \cdot 0.20 \tag{6}$$

where λ_1 = 777.41 nm, λ_2 = 777.63 nm, λ_3 = 777.75 nm.

The equivalent bandwidth (EB_{NBF}) is defined as follows:

$$EB_{NBF} = \frac{\int_{772.4}^{782.4} T_{NBF}(\lambda)d\lambda}{\overline{T_{NBF}}} \tag{7}$$

where the spectral integral bounds have been made sufficiently wide to allow the optimization of the coating design regardless of the proposed pass band shape.

The ideal NBF bandwidth would be no larger than the scientific bandwidth itself, i.e., ~0.34 nm. However, the actual bandwidth is specified ~1.9 nm to guarantee the required transmittance over the operating AOI (0° to 5.1°) range and the

temperature range (+20°C to +40°C), which can spectral shift the NBF and also considering coating manufacturing errors (coating thickness non-uniformity and CWL centering), and lifetime aging.

The out-of-band rejection requirements for the combined performance of the fully coated SRW and NBF (including substrate contributions) are specified in Table 4. The two requirements are: (1) the mean out-of-band transmittance to minimize the background signal out-of-band in the detector sensitivity range and (2) the maximum out-of-band transmittance to avoid any significant pulse spectral radiance contribution out of the required emission lines.

The Combined Out-of-Band Mean Transmittance is calculated as follows:

$$T_{OBM} = \frac{\int_{782.4}^{1100} T_{NBF} \cdot T_{SRW}(\lambda)d\lambda + \int_{200}^{772.4} T_{NBF} \cdot T_{SRW}(\lambda)d\lambda}{(1100 - 782.4) + (772.4 - 200)} \qquad (8)$$

Table 4 - Combined out of band transmittance requirements

Parameter description	Wavelength range (nm)	Value
Combined Out of Band Mean Transmittance (T_{OBM})	200 – 772.4 & 782.4 – 1100	<0.01%
Combined Out of Band Maximum Transmittance (T_{OBMax})	200 – 772.4 & 782.4 – 1100	<1%

4. OPTICAL FILTER DESIGNS

Schott BK7G18 was selected as the substrate material for the SRW and NBF filters in order to provide good thermal expansion compatibility with the optical system mounting structure while also providing good radiation resistance. For the thin film materials in the SRW and NBF filters, the SiO_2 and Ta_2O_5 material pair was chosen as it gives a good refractive index contrast and this material pair is very environmentally robust [4].

4.1 SRW design considerations

The SRW multilayer coating must reflect light over a wide wavelength range and is therefore relatively thick. Based on the required optical performance values in Table 2, the total metric thickness of the SRW filter design was ~40 µm. In addition, a two-sided design approach, which balances the coating thickness between the two surfaces, was adopted for the SRW filter to ensure compliance for the surface figure. The drawback to this balanced design approach is that it increases the risk of ghosted images.

4.2 NBF design considerations

The NBF Side A design is based on a classical multi-cavity Fabry Perot structure, where each cavity consists of two 'reflectance' stacks sandwiching a 'spacer' layer [5]. The reflectance stack consists of alternating low and high index materials, each a quarter-wave optical thickness referenced to the bandpass wavelength. The spacer layer typically consists of low or high index layers which are a multiple of a half-wave optical thickness, again referenced to the bandpass wavelength. The use of quarter-wave or half-wave optical thickness layers allows the NBF to be deposited using single wavelength monitoring (i.e., extrema monitoring). The NBF Side B design is an anti-reflection (AR) coating to maximize the NBF passband transmittance.

For this NBF filter, a complex modeling scheme was developed to track all optical performance requirements listed in Table 3 versus a wavelength shift (Figure 2). Min Tx, is the minimum transmittance in the pass band range and is an important consideration for the ghost requirement. Since absorption at the NBF CWL is minimal for the chosen substrate and material pair, the reflectance is, to first order, (1-T). The modelling indicates that the 0.45 nm NBF wavelength budget available requires relaxation of the polarization sensitivity requirement to ~0.04. Also, the ghost requirement will be met by ensuring the worst-case reflectance from the NBF Side A filter is less than 10% and the NBF Side B reflectance is less than 0.05%.
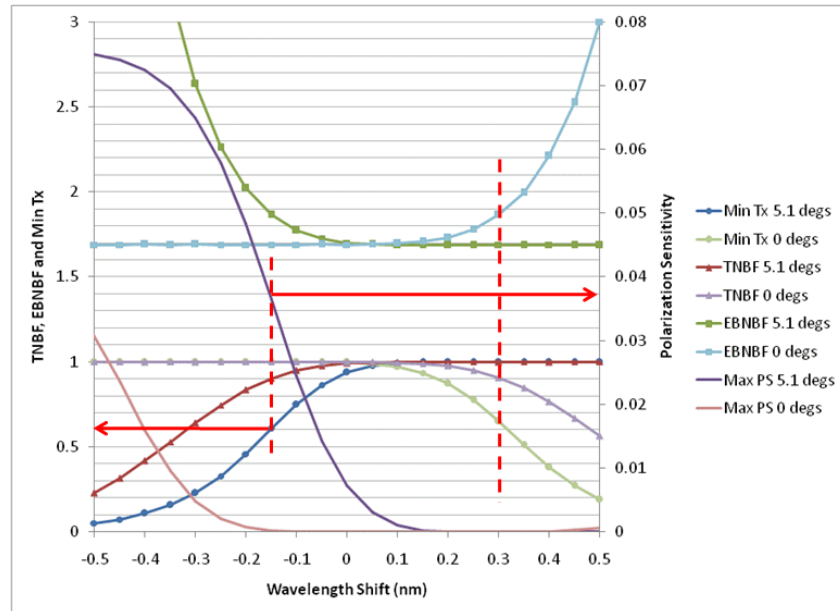
Figure 2 - Wavelength tolerancing for the optical performance requirements of the NBF

5. FILTER FABRICATION AND OPTICAL PERFORMANCE CHARACTERIZATION

Both the SRW and NBF filters were deposited using reactive magnetron sputtering deposition systems equipped with in-situ optical monitoring. The deposition and characterization challenges were very different for the SRW and NBF filters and they are described separately below.

5.1 SRW fabrication and performance

The uniformity requirements of the SRW are not as stringent compared to the NBF so that a deposition system capable of depositing on multiple SRW substrates was selected. With each deposition batch, a set of witness pieces were included to be used for later durability tests. Typically, the SRW Side A is deposited first followed by the SRW Side B.

After the completion of a SRW deposition run (Side A or Side B), the SRW filter is first inspected for surface defects such as stains, scratches and large digs to ensure that SRW coated surface passes the ISO 10110-7 surface imperfection specifications with a grade of 5/3x0.25; L2x0.02. Next, the SRW filter is spatially mapped across the surface by measuring the transmittance from 740 to 820 nm at normal incidence to provide a preliminary performance assessment and to evaluate the thickness uniformity. These normal incidence transmittance measurements can then be compared to modeled theory calculations to confirm the accuracy of the deposited multilayer coating and to ensure, indirectly, that the entire optical performance is met across the SRW clear aperture.

After both sides of the SRW filter are deposited, the SRW filter is then annealed at 225°C for several hours to accelerate the aging process and to ensure that its optical performance has a long-term (i.e., 15 years) stability based on the storage and survival temperature ranges.

The transmittance and reflectance of each SRW filter was also measured over a wavelength range from 200 to 10,000 nm at several angles of incidence between 0 and 16.3° and with s- and/or p-polarized light. Figure 3 shows the SRW transmittance and reflectance measurements over a wavelength range from 200 to 2,000 nm at an AOI of 16.3° made with a Agilent CARY 7000 spectrophotometer to validate design model. This angle was chosen as it is the largest angle required in the validation. For each SRW filter, measurements at other specified AOI's were made to confirm the agreement with design. Figure 3 shows the measured (solid curves) and calculated (dashed curves) transmittance and reflectance for both s- and p-polarized light. The wavelength range is too large to clearly see the match (or mismatch) between the measured and calculated curves, hence the wavelength range subsets shown. The agreement is generally very good, except for the reflectance in some wavelength regions as a result of beam "walk-off". What happens here is that the beam can "walk-off" to the edge of the filter due to multiple reflections between the two surfaces of the SRW
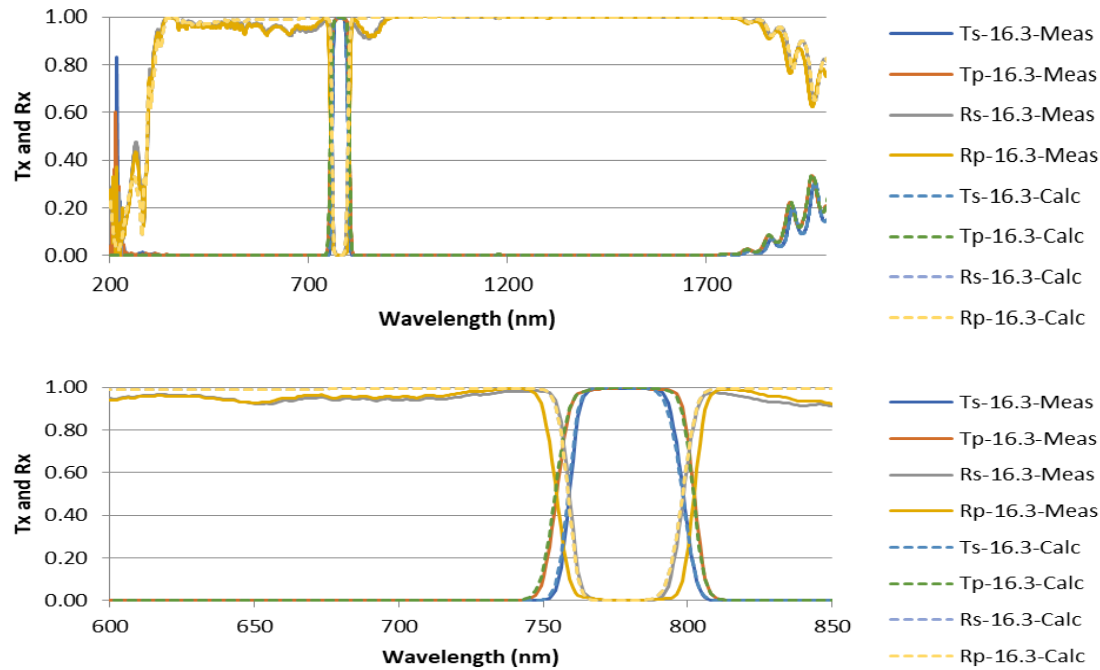
Figure 3 - SRW Measured (solid) and calculated (dashed) transmittance and reflectance curves at 16.3° for both s- and p-polarized light.

Figure 4 - Top view of a witness under test in the spectrophotometer instrument. One can see the light escaping at the edge of the substrate after bouncing back and forth from the substrate center position where it entered.

substrate, a consequence of the two-sided design. Therefore, the light at some wavelengths is 'guided' along the two surfaces until it escapes at the edge of the filter – as a result this light is not captured by the detector giving rise to a discrepancy between the measured and theoretical curves (Figure 4).

Using various measurement curves and the corresponding calculated curves, the T_{min}, TET, TER, TES, AET, AER, AEA and polarization sensitivity of the filter at 0° and 6.5° and 16.3° were estimated. In Table 5 are shown the results of these calculations which demonstrates that all the SRW filter requirements were met. The calculations assumed a 4 nm spectral band width and 3° half-cone angles, corresponding to the measurement conditions.

The uniformity of the SRW filter was evaluated from the center wavelength of the bandpass estimated at each spatially measured location. The maximum deviation over the 126-mm diameter area is +0.32% and +0.00%, respectively (±0.16%). Applying these scaling factors to the layer thicknesses of the SRW multilayer model allows the estimation of the optical performance at the extreme cases; i.e., at 0° AOI for the largest positive deviation and 16.3° AOI for the largest negative deviation. Table 6 summarizes these calculations and shows that the SRW filter meets all requirements at the extremes of the uniformity variations, temperature, and aging, over a 126-mm diameter area (which is larger than the desired 120 mm diameter effective aperture).

Table 5 - Comparison of the filter (full size) measured and calculated optical performance quantities for AOI of 0°, 6.5° and 16.3°. Measured values are shown in bold fonts.

Require-ment	Specification	0°		6.5°				16.3°			
		Meas	Calc	**Meas**		Calc		**Meas**		Calc	
		unpol	unpol	**s-pol**	**p-pol**	s-pol	p-pol	**s-pol**	**p-pol**	s-pol	p-pol
T_{min}	> 97%	**99.4%**	99.6%	**99.5%**	**99.5%**	99.6%	99.6%	**99.6%**	**99.6%**	99.6%	99.6%
TET	< 10%	**4.4%**	4.3%	**4.2%**	**4.3%**	4.2%	4.4%	**3.9%**	**4.8%**	3.9%	4.7%
TER	> 85%	---	92.1%	**91.8%**	**91.7%**	92.1%	91.92 %	**91.3%**	**90.3%**	92.5%	91.4%
TEA	< 5%	---	3.7%	**4.0%**	**4.0%**	3.7%	3.7%	**4.8%**	**4.9%**	3.6%	3.8%
AET	< 5%	**3.7%**	3.7%	---		3.6%	3.7%	---		3.6%	3.9%
AER	> 8%	**10.9%**	11.5%	---		11.6%	11.4%	---		12.1%	10.6%
AEA	< 87%	**85.4%**	84.8%	---		84.7%	84.9%	---		84.2%	85.5%
PS	< 0.5%	**NA**		**<0.1%**		<0.1%		---		0.02%	
SRW and NBF Combined	T_OBMean < 0.01%	**<0.001%**	<0.001%	**<0.001%**		<0.001%		---		---	
	T_OBMax < 1%	**<0.1%**	<0.1%	**<0.1%**		<0.01%		---		---	

Table 6 - Calculated optical performance quantities for the extremes of temperature and angle combinations, i.e. lowest temperatures (-20°C) with largest AOI (16.3°) and highest temperature (+80°C) with smallest AOI (0°).

Characteristic checked	Specification	AOI = 0°		AOI = 16.3°	
		No change	+0.22% at 80°C	-0.0% at 20°C	
		s-pol	s-pol	s-pol	p-pol
Tmin	> 97%	99.6%	99.6%	99.7%	99.7%
TET	< 10%	4.3%	4.3%	3.9%	4.7%
TER	> 85%	92.0%	92.0%	92.5%	91.4%
TEA	< 5%	3.7%	3.7%	3.6%	3.9%
AET	< 5%	3.7%	3.7%	3.6%	3.9%
AER	> 8%	11.5%	11.5%	12.1%	10.6%
AEA	< 87%	84.8%	84.8%	84.2%	85.5%

5.2 NBF fabrication and performance

The Side B of the NBF filter is deposited on the same deposition platform used to deposit the SRW Side A and Side B coatings. As mentioned previously, the NBF Side B design is an AR coating and it does not have stringent uniformity requirements as it is intended to maximize the NBF passband transmittance.

The Side A of the NBF filters does have stringent uniformity requirements over the NBF effective aperture. In order to achieve this uniformity, a different deposition platform was selected that can coat only one NBF filter at a time (along with the required witness pieces for later durability tests). With the quarter-wave/half-wave design structure of the Fabry-Perot filter (with FWHM ~ 1.4 nm), it is possible to use a single wavelength extremum monitoring method which has a well-known automatic error compensation mechanism to allow over/under-shoots in the thickness of one layer to be compensated by the following layer [5,6]. The uniformity of the deposited coating was optimized by fine-tuning the deposition geometry of the deposition. Great care was taken when loading a NBF substrate into the deposition chamber to achieve a reproducible substrate placement relative to the targets and to minimize substrate wobble (which can affect azimuthal uniformity).
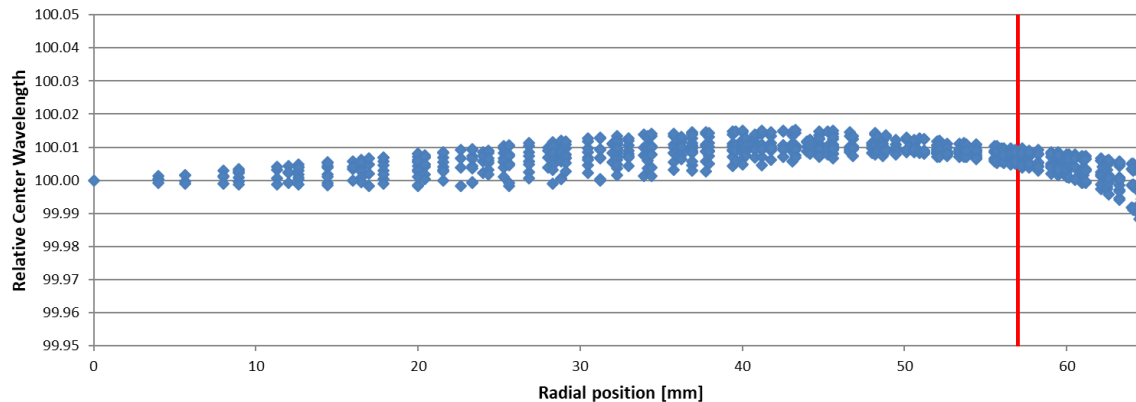
Figure 5 - NBF Filter - Normalized-CWL versus radial position distribution over the full effective area of the filter, post anneal-tuning and edging. The red line indicates the edge of the effective area.

The optical monitoring was performed with a laser operating at a wavelength slightly lower than the required passband CWL at room temperature. This allowed the CWL of the NBF filter to be fine-tuned by annealing the filter in a controlled manner. This annealing step also improves the long-term stability as previously described for the SRW filter.

The transmittance measurements for the NBF are challenging because of the narrowness of the bandpass and instruments with superior spectral and angular resolution are needed to correctly measure the transmittance peak shape. Typically, instruments that can achieve such spectral and angular resolution are usually limited to normal incidence and unpolarized transmittance measurements. However, with these instruments it is possible to accurately "map" the entire filter area and assess the distribution of the optical performance over the filter effective aperture, and calculate tolerances based on 'shift-width' estimations (see below) for all other operating conditions. To verify these results, other measurements are performed at oblique AOI's, over wider wavelength ranges and at different temperatures but only on a witness pieces or at a single location on the filter.

The normal angle transmittance measurements were made on the NBF filter using a 4 mm x 4 mm grid step pattern. From this, a subset of the above spatially mapped measured points is then used to evaluate the uniformity and the 'shift-width' analysis: i.e., those located at every 10 mm along radial lines separated by 30° each, resulting in a total of 69 points after eliminating overlapping measurement points near the center of radius.

Figure 5 presents the center wavelength (CWL) values obtained from the 4 mm x 4 mm grid step mapped points based on their radial distance. The CWL values were normalized to the value obtained at the center of the substrate (radius of 0 mm). The red line in the chart indicates the edge of the effective aperture ($\varnothing$114 mm). Up to a radius of 57 mm, the effective aperture limit, the highest and lowest values are separated by 0.014%, so the NBF CWL uniformity is ±0.007% over the effective aperture.

To determine whether an NBF filter is passing or failing based on 0°-incidence measurements, the following three-step methodology ("shift-width" analysis) was carried out:

1. **Find the maximum down-shift and up-shift possible:**

   Wavelength shifts all 69 points to determine the wavelength range, or shift width, over which the entire filter area (all 69 points) passes both T_{NBF} and EB_{NBF}, i.e.:

   a. Shift the performance of the 69 measurements down in wavelength until 1 of the 69 points starts to fail: this gives $\Delta\lambda_{min}$ (a negative number);
   b. Shift the performance of the 69 measurements up in wavelength until 1 of the 69 points starts to fail: this gives $\Delta\lambda_{max}$ (a positive number);
   c. Calculate the total starting shift width with $\Delta\lambda_{tot} = \Delta\lambda_{max} - \Delta\lambda_{min}$

2. **Wavelength budget:**

   The $\Delta\lambda_{min}$ and $\Delta\lambda_{max}$ are now adjusted to consider the filter operating conditions as follows:

a. Angle tuning shift is -0.762 nm from 0 to 5.1° AOI (verified experimentally): changes
$\Delta\lambda_{min} \rightarrow \Delta\lambda_{min} + 0.762$nm;

b. Lifetime aging (over) estimated to $+0.010$ nm: changes $\Delta\lambda_{max} \rightarrow \Delta\lambda_{max} - 0.010$ nm

c. Thermal shift is $+3.5$ pm/°C (verified experimentally): changes both $\Delta\lambda$min and $\Delta\lambda$max based on the
measurement temperature (T_m):
   - $\Delta\lambda_{min} \rightarrow \Delta\lambda_{min} + (T_m - 20) * 0.0035$
   - $\Delta\lambda_{max} \rightarrow \Delta\lambda_{max} + (T_m - 40) * 0.0035$

3. Filter evaluation:

The adjusted shift width $\Delta\lambda_{tot}$ is now calculated from the corrected $\Delta\lambda_{min}$ and $\Delta\lambda_{max}$ values:
$\Delta\lambda_{tot} = [\Delta\lambda_{max} - 0.010 + (T_m - 40) * 0.0035] - [\Delta\lambda_{min} + 0.762 + (T_m - 20) * 0.0035] = \Delta\lambda'_{max} - \Delta\lambda'_{min}$ (note the
added the "prime" symbol)

Whether the NBF filter now passes or not is determined by the following:

a. If $\Delta\lambda_{tot} < 0$ then the filter fails

b. If $\Delta\lambda_{tot} > 0$ then
   - If $\Delta\lambda'_{max} < 0$ then the filter is too high in wavelength and the filter fails;
   - If $\Delta\lambda'_{max} > 0$ then the filter is too low but can be annealed up in wavelength;
   - If $\Delta\lambda'_{min} < 0$ and $\Delta\lambda'_{max} > 0$ then the filter passes. Additional tuning anneal can potentially be done to optimize performance.

This process can be repeated for different values of T_{NBF} and EB_{NBF} to determine the best performance that the filter area can meet. It is important to note that any variability in the peak transmittance and bandwidth is considered when performing the shift width analysis over the entire area of the filter.

For the filter shown in Figure 6, over the 69-point grid, all points are simultaneously passing T_{NBF} (>87%) and EB_{NBF} (<1.94 nm). Note that Figure 6 shows all 69 curves with the two extremes, corresponding to the lowest and highest wavelength on the measured filter area, highlighted in red.

From this measurement it was determined that the maximum negative shift ($\Delta\lambda_{min}$) was -0.042 nm and the maximum positive shift width ($\Delta\lambda_{max}$) was +0.096 nm after correcting for angle tuning, lifetime aging and operating temperature from +20 to +40°C. Therefore, the filter area has a shift width of 0.138 nm. This shift width is a measure of the wavelength tolerance on the part. These values have an uncertainty of approximately ±0.010 nm.
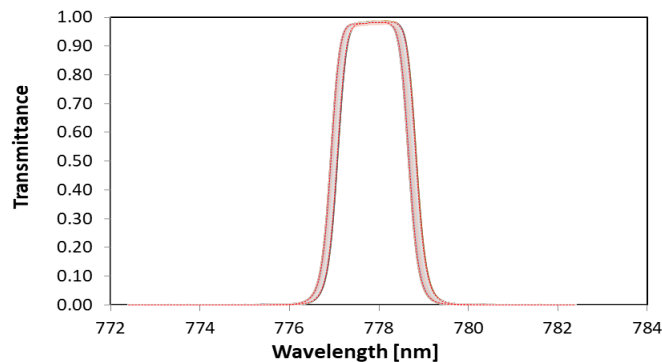
Figure 6 - Transmittance curves for one QM NBF filter from the 69 points map with highest and lowest measured wavelength measured curve.

6. STABILIZATION AND TUNING WITH ANNEALING

Sputtered oxide coatings typically age by diffusion mechanisms and are thermally activated. The changes seen are both in metric layer thickness and refractive index. For bandpass filters made from SiO_2/Ta_2O_5, the coating designs are such that during annealing (at temperatures higher than the deposition temperature), the wavelength increases (shifts on the order of 1 to 2 nm) while the transmittance level remains unaffected.

The wavelength shift, a thermally activated process, can be modelled based using an Arrhenius rate equation:

$$\Delta CWL = f(t)\exp(-E_a/kT)$$ (9)

where $f(t)$ is a time dependence function, E_a an activation energy, k the Boltzmann's constant and T the temperature in Kelvin. Through annealing experiments, $f(t)$ and E_a can be determined for the NBF and SRW filters. From this, one can then calculate the minimum annealing time required at a given annealing temperature to guarantee that the filter will move less than 0.002 nm when stored at +90°C. It is also possible to use this approach to predict the wavelength shift of a filter if annealed at an elevated temperature for a given time; this allows the CWL of a filter to be fine-tuned to within picometers (pm) of a target CWL.

After the completion of both Side A and Side B deposition runs, the NBF filter is first annealed a minimum of 6 hours at 225°C to ensure stable wavelength positioning to within 10 pm over a minimum of 15 years.

7. FILTER ENVIRONMENTAL DURABILITY

The NBF and SRW filters have been tested for various environmental conditions and have shown no perceptible changes in optical performance and no apparent physical deterioration or discoloration.

A list of all the tests is given below. Note that these tests were always performed on a set of witness pieces from each coating batch and at least once on actual qualification models (full size filters):

- Solubility: acetone and then ethanol, 5 minutes each time
- Mild abrasion: cheese cloth rubbing, 50 strokes, 50N pressure
- Adhesion: tape test, remove in one stroke in ~1s
- Humidity exposure: 48 h at 55°C and >95% RH
- SRW thermal vacuum cycling: -110°C and +160°C, 30 min dwell time, 30 cycles
- NBF thermal vacuum cycling: -90°C and +90°C, 30 min dwell time, 30 cycles

After each test, the witness surfaces were inspected for any evidence of physical damage. Once all tests were completed the filter optical performance were measured again to verify there was not significant change.

Radiation testing was also performed on witness samples:
- Proton radiation – 2 MeV (NIEL 3.3×10^{-2} MeV cm^2/g):
  - SRW: up to 1.9×10^{13} p$^+$/cm^2 (TNID 6.3×10^{11} MeV/g)
  - NBF: up to 4.1×10^9 p$^+$/cm^2 (TNID 1.34×10^8 MeV/g)
- Gamma radiation – Cobalt 60$^+$
  - NBF: up to 600 krad
- Combined electron and solar UV radiation
  - SRW: ~1500 equivalent sun hours (ESH) of combined VUV, UV and a 1 keV plus 10 keV electron fluence of ~1.5×10^{16} e$^-$/cm^2.

After these radiation tests, the witness pieces were re-measured optically. Some very minor absorption was detected in the UV range of the SRW samples after the combined electron and UV solar radiation exposure. It is not known yet if this minor absorption increase in the UV spectral range can be attributed to the substrate material or the coating materials (or both) nor which of the radiation tests (VUV, UV, 1 keV or 10 keV electrons) may have caused this deterioration.

In addition, air-to-vacuum testing was also performed. With reactive magnetron sputtering, the deposited films are very dense (hence free of porosity or voids) so they do not absorb water vapour when exposed to air which would otherwise affect their refractive index. This can be verified by exposing the films to vacuum and looking for a wavelength shift. Tests were carried out with both SRW and NBF witness sample loaded into a cryostat mounted inside the sample

compartment of a spectrophotometer. Within the accuracy of the measurement, there was no wavelength shift in the filter when a filter transitioned from air to vacuum to air. Note that the samples were kept in air or vacuum for a minimum of 3 days each time to ensure the coating would have time to absorb or desorb water vapor. Also note that great care was taken to maintain the sample at constant temperature, to within 0.1°C, to ensure the sample would not shift in wavelength because of its temperature coefficient.

8. CONCLUSION

The Lightning Imager will be the first instrument developed in Europe (and Canada) for the detection of lightning events from geostationary orbit. The challenging detection requirements in day and night conditions, combined with the large earth coverage and the tight mass and spatial envelope make the Lightning Imager a complex instrument from an optical perspective.

Despite the complexity of the requirements, an instrument based on four simple dioptric lenses has been designed that employs a SRW and NBF filter on each optical path. The SRW filters must survive heavy radiation exposure and direct sunlight and they are required to reflect most of the sunlight in order to increase the LI's signal-to-noise ratio. The NBF filters have very challenging uniformity requirement across a 114 mm diameter area, combined with a requirement for a maximized weighted transmittance from 777.41 to 777.75 nm.

As demonstrated above, both the SRW and NBF filters have been successfully manufactured, and through extensive characterization tests, have been shown to meet all the stringent requirements imposed upon them.

REFERENCES

[1] Meteosat Third Generation (MTG), EUMETSAT,
https://www.eumetsat.int/website/home/Satellites/FutureSatellites/MeteosatThirdGeneration/index.html
[2] J. Grandell, "Meteosat Third Generation (MTG): Lightning Imager and its products,"
http://www.eumetrain.org/data/3/362/362.pdf
[3] S. Lorenzini, R. Bardazzi, M. Di Giampietro, F. Feresin, M. Taccola, and L. Perez Cuevas, "Optical design of the Lightning Imager for MTG," Proc. of SPIE Vol. 10564 1056406-2 (2012).
[4] S. M. Edlou, A. Smajkiewicz, and G.A. Al-Jumaily, "Optical properties and environmental stability of oxide coatings deposited by reactive sputtering," Appl. Opt. 32, 5601 (1993).
[5] H. A. Macleod and H. A. Macleod. Thin-film optical filters. Boca Raton: CRC press, 2010.
[6] B. T. Sullivan and G. Carlow, "An overview of optical monitoring techniques," in *Optical Interference Coatings, OSA Technical Digest* (Optical Society of America, 2010), paper TuC1.